

10/92950

SLAC-PUB--5678

DE92 004948

Large Acceptance Magnetic Spectrometers for Polarized Deep Inelastic Electron Scattering*

G. G. Petratos, R. L. Eisele, R. A. Gearhart, E. W. Hughes, and C. C. Young
Stanford Linear Accelerator Center, Stanford University, Stanford, CA 94309

Abstract

The design of two magnetic spectrometers for the measurement of the spin-dependent structure function g_1^n of the neutron and a test of the Bjorken sum rule is described. The measurement will consist of scattering 23 GeV polarized electrons off a polarized ^3He target and detecting scattered electrons of 7 to 18 GeV at 4.5° and 7° . Each spectrometer is based on two large aperture dipole magnets bending in opposite directions. This "reverse" deflection design doubles the solid angle as compared to the conventional design of same direction bends used in previous experiments. Proper choice of the deflection angles and the distance between the two dipoles in each spectrometer allows background photons from radiative processes to reach the detectors only after at least two bounces off the spectrometer vacuum walls, resulting in an expected tolerable background. Each spectrometer is equipped with a pair of Čerenkov detectors, a pair of scintillation hodoscopes and a lead-glass shower calorimeter providing electron and pion identification with angular and momentum resolutions sufficient for the experimental measurement.

MOTIVATION

This paper describes the design of two magnetic spectrometers to be used in an experiment [1] at the Stanford Linear Accelerator Center that will (a) measure the spin-dependent structure function $g_1^n(x)$ of the neutron in the Bjorken scaling variable x from 0.035 to 0.7 with squared four-momentum transfers $Q^2 > 1$ (GeV/c) 2 and (b) test the Bjorken polarization sum rule [2]:

$$\int_0^1 [g_1^p(x) - g_1^n(x)] dx = \frac{1}{6} \left| \frac{g_A}{g_V} \right| \left[1 - \frac{\alpha_s(Q^2)}{\pi} \right], \quad (1)$$

where $g_1^p(x)$ is the proton spin-dependent structure function, α_s is the QCD coupling constant and $|g_A/g_V|$ is the ratio of the axial to vector weak coupling constants in the nucleon beta decay. The experiment is also expected to provide valuable information in understanding the violation of the Ellis-Jaffe quark parton model sum rule [3] as measured by the EMC collaboration [4].

THE EXPERIMENT

The experiment consists of scattering a 22.7 GeV longitudinally polarized electron beam off a polarized ^3He (neutron) target [5] and detecting scattered electrons in

two magnetic spectrometer systems. The neutron spin structure function g_1^n is proportional to the difference over the sum of the scattering cross sections in which the beam and target polarizations are parallel versus anti-parallel. The beam polarization will be measured by means of a Möller polarimeter [6] and the target polarization by two NMR techniques [5,7].

THE MAGNET SYSTEMS

The two spectrometers will be centered around 4.5° and 7.0° , which are the optimum scattering angles corresponding to the maximum polarized electron beam energy of 22.7 GeV, presently available at the SLAC fixed target End Station A facility. A momentum acceptance ranging from 7 to 18 GeV/c is required at these angles to cover the desired range in the Bjorken x scaling variable from 0.035 to 0.7. A schematic of the two systems is shown in Fig. 1. Both systems use magnetic elements from the SLAC 8 and 20 GeV/c spectrometers and standard surplus concrete blocks for background shielding.

The design of the two systems was driven by several requirements. The cross sections to be measured are known to be small, typically of the order of 10^{-32} cm 2 /(sr·GeV). The asymmetry in the cross sections of the two different spin orientations is also predicted to be small, of the order of 10^{-3} . In order to minimize beam running time, the spin structure function measurements require spectrometers with the largest possible solid angle over a momentum acceptance range extending from 7 to 18 GeV/c.

In addition, these small scattering angle spectrometers should be able to suppress an expected large photon background coming from the target due to bremsstrahlung radiation, radiative Möller scattering and the decay of photoproduced π^0 mesons. Background rate estimates [8] have indicated the need for at least a "two bounce system" (the shape of the spectrometer aperture should allow a photon to reach the detectors only after bouncing twice on the magnet gaps or vacuum walls) in order to keep this background at a tolerable level.

The momentum resolution of the spectrometers is defined solely by the required x resolution. The cross section asymmetries are not expected to exhibit any sizable dependence on momentum transfer [4]. A resolution in x ranging from ± 0.004 at $x=0.035$ to ± 0.07 at $x=0.7$ ($\Delta x/x = \pm 0.10$) is considered adequate for the needs of the asymmetry measurements. This translates to a required momentum resolution that varies from $\pm 6.9\%$ at $E'=7$ GeV/c to $\pm 2.2\%$ at $E'=18$ GeV/c for both spectrometers.

Past designs for polarized deep inelastic scattering experiments at SLAC [9,10] have achieved a solid angle

* Work supported by Department of Energy contracts DE-AC03-76SF00515.

MASTER

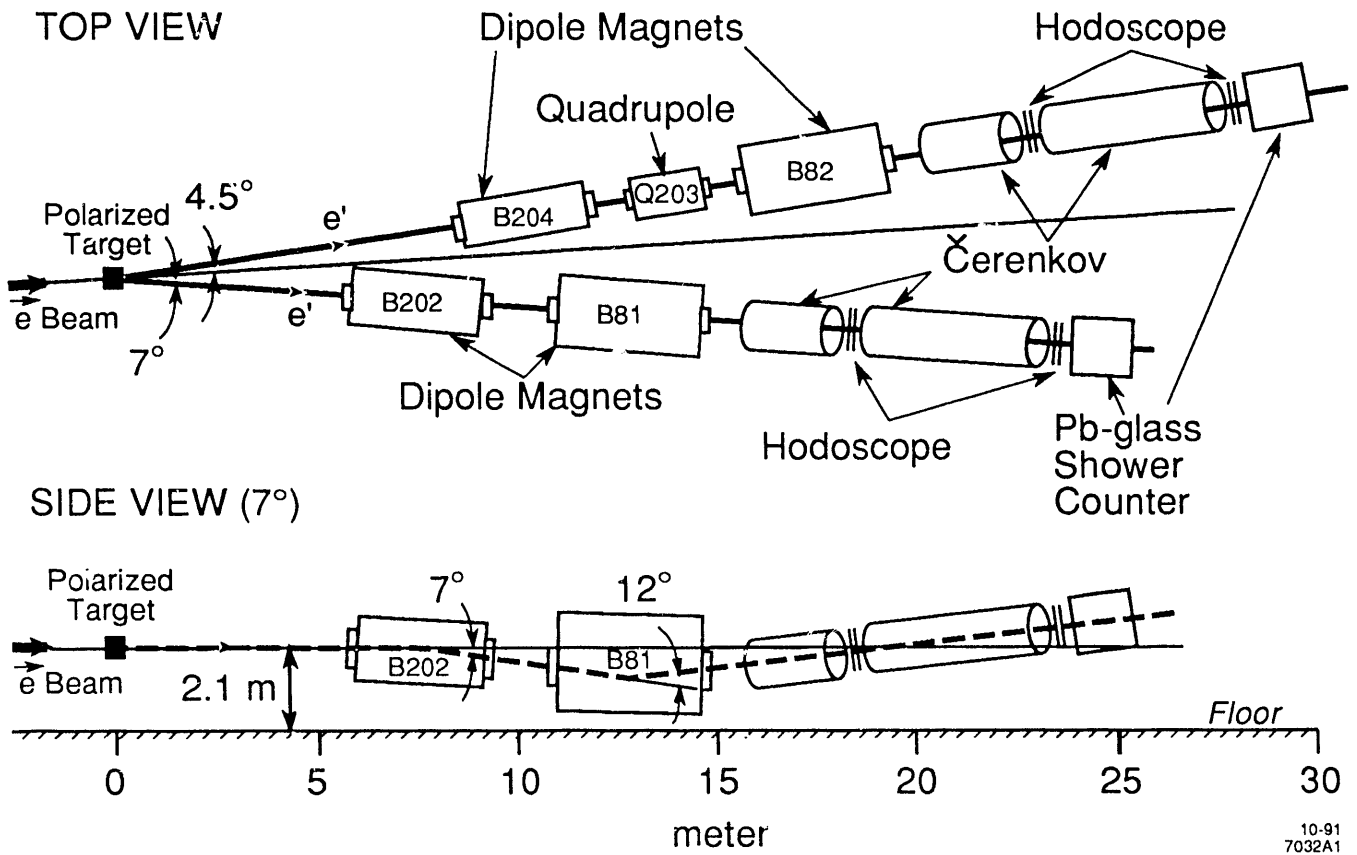


Fig. 1. The two magnetic spectrometer systems and detector packages. The dipoles B202 and B204 and the quadrupole Q203 are magnetic elements from the SLAC 20 GeV/c spectrometer. The dipoles B81 and B82 are elements from the SLAC 8 GeV/c spectrometer. Not shown is a set of wire chambers in the 4.5° arm and/or a third hodoscope in both arms (under consideration).

peaking at a maximum value of ~ 0.6 msr for the central momentum but falling rapidly on either side of the relative momentum. The designs were based on two large aperture dipole magnets both bending in the same direction. A new design with the two dipoles bending in opposite directions provides a solid angle peaking at the same maximum but remaining constant over a large momentum interval $\Delta E'/E' \sim 100\%$. The solid angle of the "reverse bend" dipole doublet configuration, when integrated over the 7 to 18 GeV/c momentum interval, is twice that of the "conventional" configuration. The solid angle of the two spectrometers is shown as a function of momentum in Figs. 2 and 3.

The reverse bend can also fulfill the "two bounce" requirement by properly choosing the deflecting angles and the separation of the two dipoles. In the 7.0° spectrometer the distance between the two dipoles was chosen to be 2 m and the two deflection angles 7° for B202 and 12° for B81. This combination makes the spectrometer a "two bounce" system for photons and at the same time provides sufficient total dispersion for determining the scattered particle momenta. In the 4.5° arm the deflection angles of the dipoles are the same as for the 7.0° arm but their separation is 4 m resulting in an almost "three bounce" system.

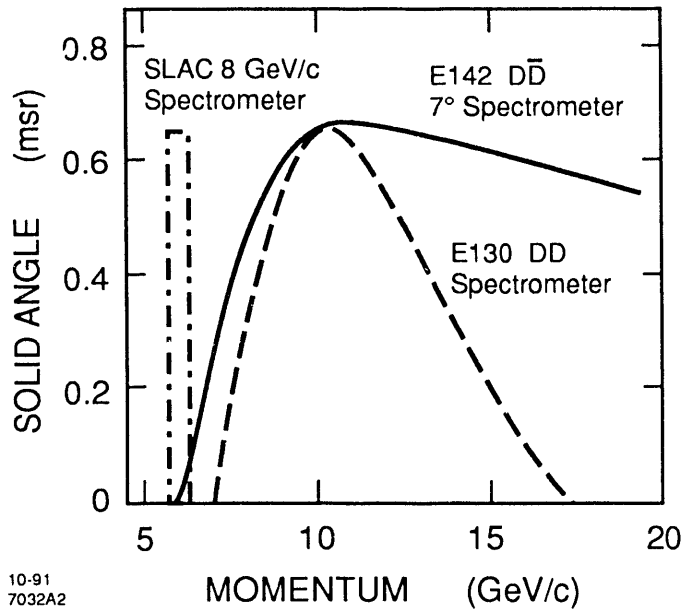


Fig. 2. The solid angle of the 7.0° magnetic spectrometer system plotted versus momentum. The acceptances of the E130 spectrometer and of the SLAC 8 GeV/c spectrometer are shown for comparison.

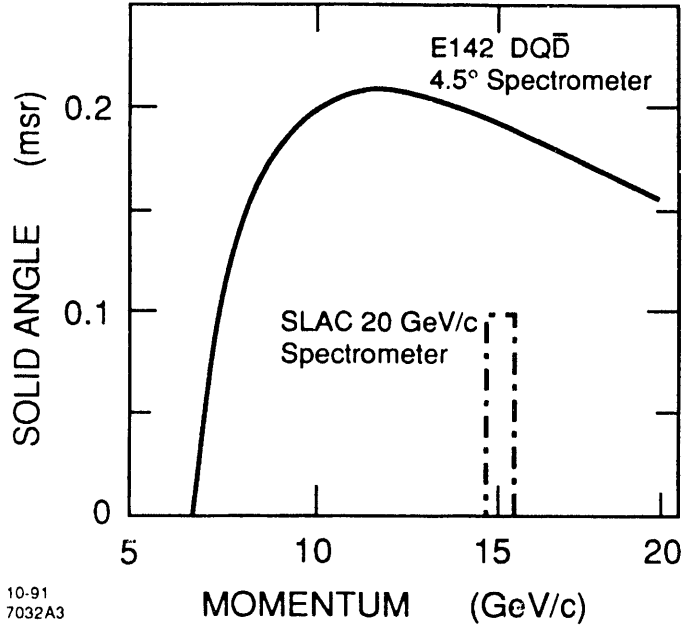


Fig. 3. The solid angle of the 4.5° magnetic spectrometer system plotted versus momentum. The acceptance of the SLAC 20 GeV/c spectrometer is shown for comparison.

Another advantage of the reverse bend configuration is that the detector package is located at approximately the primary beam height. This convenient elevation makes the concrete structure required for shielding the detectors from room background considerably less massive compared to the conventional design with both dipoles bending up. The reduced mechanical complexity translates to significant economic benefits as both the set-up time and apparatus costs are minimized.

In the reverse bend design, the bend plane position of the scattered particles at the detectors depends weakly on their momenta as can be seen in Fig. 4. The particle momenta are correlated with the divergence of their trajectory at the exit of the spectrometer. This results in a loss in momentum resolution, not critical to the experiment, but spreads out the pion background, which is highly peaked at 7 GeV/c, onto a large detector area, allowing measurements at a fairly large pion rate.

The purpose of the quadrupole in the 4.5° spectrometer is to increase the angular magnification in the non-bend plane and spread the scattered particles onto a larger detector area in this direction as can be seen in Fig. 5. In the bend plane the quadrupole focusing improves the momentum resolution of the system as both the position and divergence of the scattered particles at the exit of the spectrometer are correlated with momentum. The introduction of the quadrupole reduces the highly peaked solid angle in the range of 7 to 10 GeV/c and relaxes the instantaneous counting rates in the detectors allowing accumulation of data in parallel and at the same rate with the 7° spectrometer.

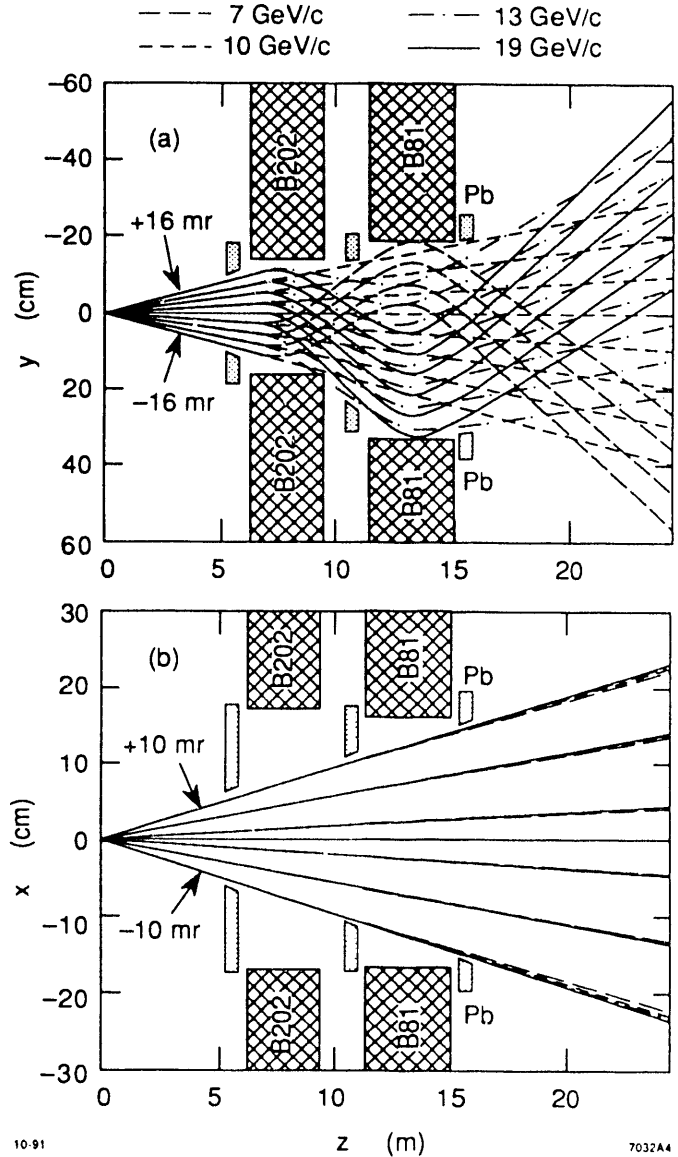


Fig. 4. Raytrace for the 7° spectrometer for rays of different momenta originating from the center of the polarized target. All rays are drawn with respect to the central trajectory of the system ($\phi_0 = \theta_0 = 0$ mr, $E' = 10$ GeV/c). Also shown are the iron magnet poles and lead collimators. Top: bend plane; bottom: non-bend plane.

THE DETECTORS

Each spectrometer will be instrumented with a pair of gas threshold Čerenkov detectors [11], a pair of finely segmented scintillator hodoscopes [12] and a segmented lead-glass calorimeter of 24 radiation lengths in a fly's eye arrangement [13]. The electrons will be distinguished from the large pion background using the pair of gas threshold Čerenkov counters in coincidence. The pair of hodoscopes will provide tracking information as well as timing information to assist in pion rejection.

The scattered electron energy will be measured by two methods. The first one will use the track information from the two hodoscopes and the known optical properties of

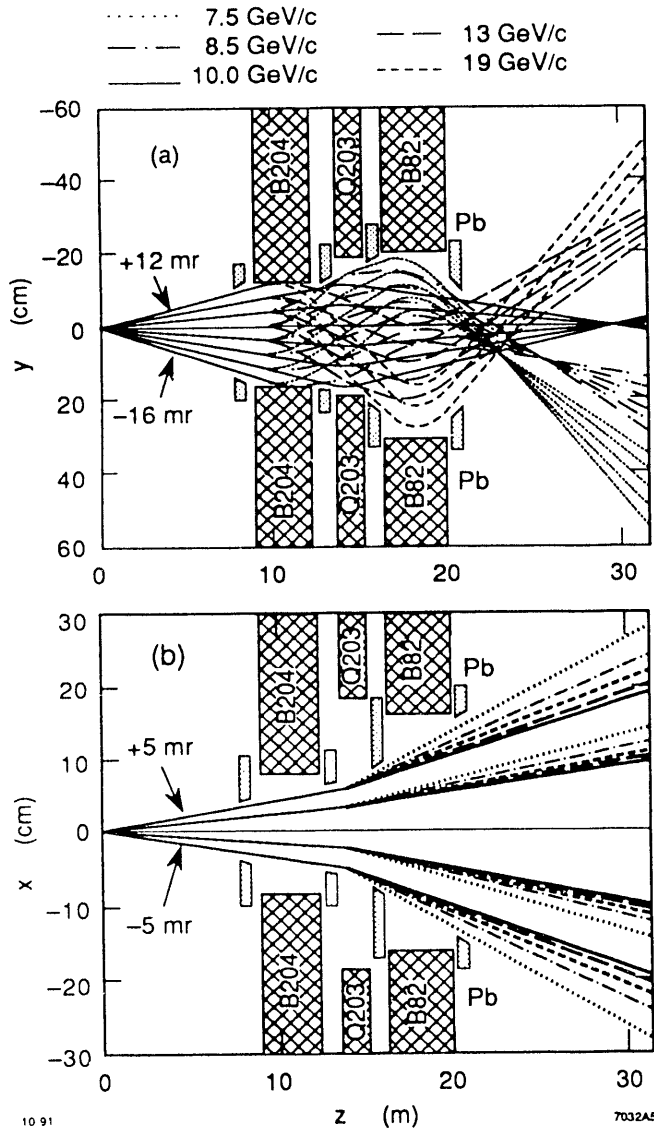


Fig. 5. Raytrace for the 4.5° spectrometer for rays of different momenta originating from the center of the polarized target. All rays are drawn with respect to the central trajectory of the system ($\phi_0 = \theta_0 = 0$ mr, $E' = 10$ GeV/c). Also shown are the iron magnet poles and lead collimators. Top: bend plane; bottom: non-bend plane.

the magnetic spectrometer. The second one will rely on the energy deposited in the lead-glass calorimeter. The scattering angle is measured with very good resolution by using the hodoscope track information. The fine segmentation of the shower counter can also provide a measurement of the scattering angle with resolution sufficient for the needs of the experiment.

Each shower counter calorimeter will be assembled by a subset of 200 blocks of the lead-glass package [14] of the ASP experiment at the PEP ring. The blocks will be arranged in a fly's eye configuration with a segmentation that will allow accumulation of data at a maximum π/e ratio of about 20. With the two Čerenkov counters in the

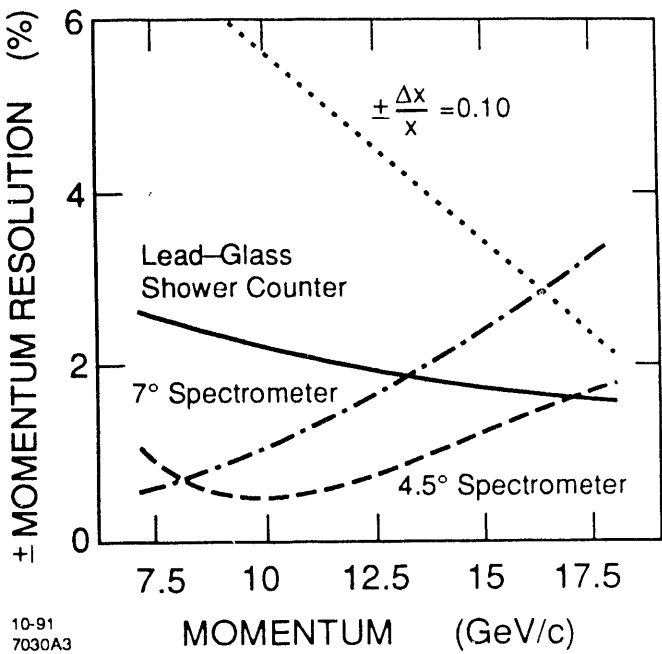


Fig. 6. Expected momentum resolution of the two magnetic spectrometer systems. Also shown is the expected energy resolution of the reconfigured ASP lead-glass shower counter as well as the required momentum resolution that corresponds to the desired x resolution.

trigger, the contamination of the shower signals by pions is expected to be very small.

The two Čerenkov counters of each spectrometer, 2 and 4 m in length, employ CO_2 radiator gas because of its properties of low scintillation and low cross sections for knock-on electrons created by the passage of pions. The 2 m Čerenkov counter will operate at a threshold for light production by pions of 9 GeV/c and the 4 m Čerenkov counter at a threshold of 13 GeV/c. The expected number of photoelectrons per incident electron is calculated to be, after taking into account all losses, greater than 7.5, resulting in a detection efficiency over 99.5%.

The two scintillator hodoscopes will provide data for a statistical evaluation of possible systematic errors in the lead-glass and Čerenkov counter data. They are expected to be instrumental in pion identification for measuring also the asymmetry of inclusive pion yields, which is another physics goal of the experiment.

The fine segmentation of the hodoscopes (there are ~ 140 scintillator elements per spectrometer) was chosen to tolerate the large expected photon and neutron backgrounds and to reconstruct with sufficient resolution the production coordinates of the scattered particles. Both horizontal and vertical planes consist of scintillator elements of 3 cm width with a "2/3" overlap resulting in a bin width of 1 cm. The separation of the two hodoscopes will be ~ 6.5 m in the 4.5° arm and ~ 4.5 m in the 7.0° arm.

RESOLUTIONS

The shower counter resolution for electrons should be about $\sigma/E' \approx \pm 7\%/\sqrt{E'}$. This estimate will result in a energy resolution $< \pm 2.5\%$, adequate for the needs of this experiment. The counter will be calibrated with a sample of scattered electrons of known energy in special elastic electron-proton scattering runs using a gaseous hydrogen target. The energy of the scattered electrons in these runs will be ~ 5 GeV. Extrapolation of the calibration algorithm to higher energies will be checked using the scintillator hodoscopes.

The angular tracking resolutions of the hodoscopes are ± 0.7 mr for the 4.5° spectrometer and ± 0.9 mr for the 7.0° spectrometer; the position tracking resolutions are ± 0.3 cm for both spectrometers. The expected angular resolutions in the non-bend plane are $\sim \pm 0.3$ mr for both spectrometers. In the bend plane, they are $\sim \pm 0.9$ mr for the 4.5° arm and $\sim \pm 0.3$ mr for the 7° arm.

The momentum resolution depends on the absolute value of momentum and varies from $\pm 0.5\%$ to $\pm 1.8\%$ for the 4.5° spectrometer and from $\pm 0.6\%$ to $\pm 3.5\%$ for the 7.0° spectrometer as can be seen in Fig. 6. The figure also shows the projected energy resolution of the reconfigured ASP shower counter as well as the required momentum resolution that corresponds to the desired Bjorken x resolution. The angular and momentum spectrometer resolutions, averaged over the 7 to 18 GeV/c range, are given for both systems in Table 1.

The initial (at the target) production coordinates χ_0 , θ_0 , y_0 and ϕ_0 and the momentum of the particles transported through the spectrometers will be reconstructed by means of reverse-order TRANSPORT matrix elements [15] using the final (at the second hodoscope location) χ_f , θ_f , y_f and ϕ_f coordinates of the particles. The very large momentum bites of the spectrometers require at least a third-order reverse TRANSPORT expansion in y_f and ϕ_f for reconstructing the particle momenta as can be seen in Figs. 7 and 8. The angular coordinates θ_0 and ϕ_0 are well reconstructed by a second-order reverse expansion in terms of the final coordinates.

SUMMARY AND OUTLOOK

The reverse bend design generally is a practical, efficient configuration for low resolution experiments that require high momentum (> 10 GeV/c) spectrometers maintaining a large solid angle over a large momentum range.

Another experiment using the two spectrometer systems is being proposed [16] at SLAC for measuring deep inelastic scattering of 25.9 GeV polarized electrons from polarized ammonia (NH_3) and deuterated ammonia (ND_3) targets. The same spectrometer design could be used in the polarized experiments possible with a planned [17] upgraded beam energy of 50 GeV.

ACKNOWLEDGMENTS

We wish to acknowledge the invaluable support of Sylvia MacBride, Vani Bustamante and Kevin Johnston from the SLAC Publications Department in this work.

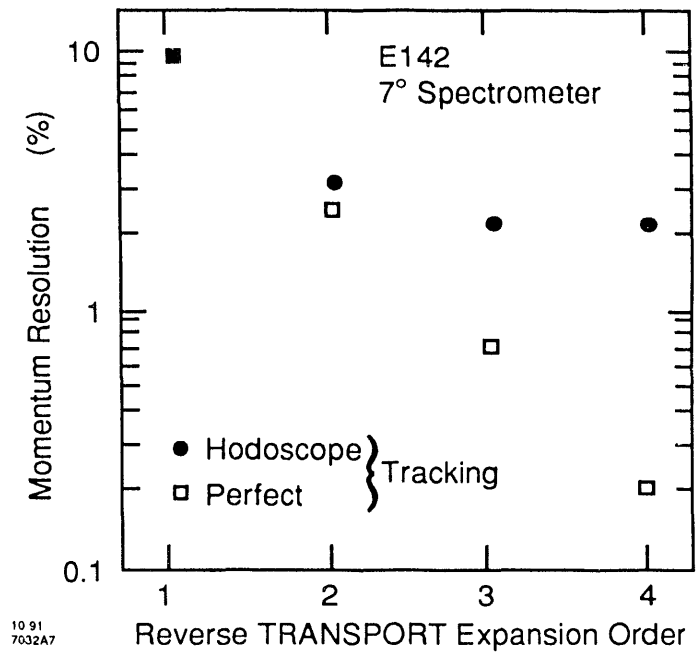


Fig. 7. Average momentum resolution of the 7° spectrometer system versus the order of the reverse TRANSPORT set of matrix elements. Shown is the intrinsic resolution assuming perfect tracking and the resolution using the track information from the two hodoscopes.

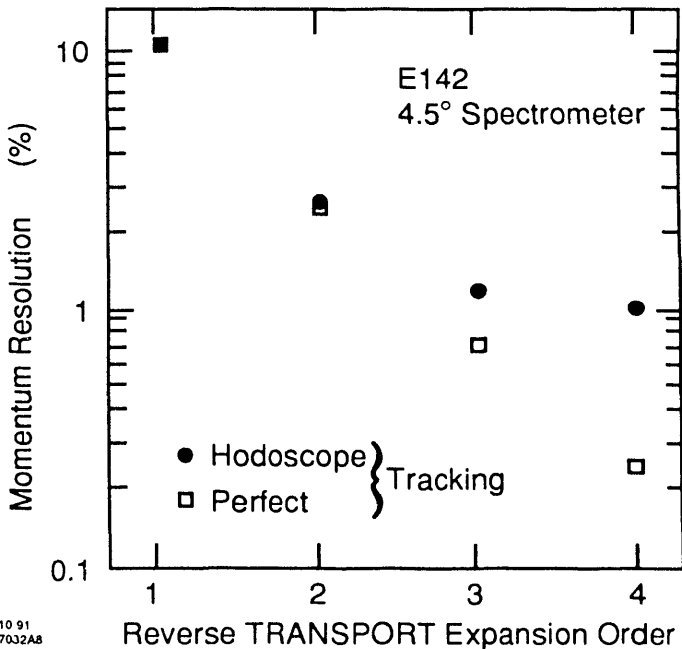


Fig. 8. Average momentum resolution of the 4.5° spectrometer system versus the order of the reverse TRANSPORT set of matrix elements. Shown is the intrinsic resolution assuming perfect tracking and the resolution using the track information from the two hodoscopes.

Table 1. Momentum and angular resolutions, averaged over a 7 to 18 GeV/c range, using third-order (second-order) reverse matrix elements for momentum (angle) reconstruction.

7° Spectrometer

RESOLUTION	Intrinsic	Hodoscope Tracking
Momentum	± 0.7 %	± 2.2 %
Bend Plane Angle ϕ_0	± 0.2 mr	± 0.3 mr
Non-bend Plane Angle θ_0	0 mr	± 0.3 mr

4.5° Spectrometer

RESOLUTION	Intrinsic	Hodoscope Tracking
Momentum	± 0.6 %	± 1.2 %
Bend Plane Angle ϕ_0	± 0.7 mr	± 0.9 mr
Non-bend Plane Angle θ_0	0 mr	± 0.3 mr

REFERENCES

- [1] E. W. Hughes *et al.*, "SLAC Proposal E142: A Proposal to Measure the Neutron Spin-Dependent Structure Function" (1989).
- [2] J. D. Bjorken, "Applications of the Chiral $U(6) \otimes U(6)$ Algebra of Current Densities," *Phys. Rev.* **148**, pp. 1467–1478, 1966; "Inelastic Scattering of Polarized Leptons from Polarized Nucleons," *Phys. Rev.* **D1**, pp. 1376–1379, 1970.
- [3] J. Ellis and R. L. Jaffe, "A Sum Rule for Deep Inelastic Electroporation for Polarized Protons," *Phys. Rev.* **D9**, pp. 1444–1446, 1974.
- [4] J. Ashman *et al.*, "An Investigation of the Spin Structure of the Proton in Deep Inelastic Scattering of Polarized Muons on Polarized Protons," *Nucl. Phys.* **B328**, pp. 1–35, 1989.
- [5] T. E. Chupp *et al.*, "Polarized, High-Density, Gaseous ^3He Targets," *Phys. Rev.* **C36**, pp. 2244–2251, 1987.
- [6] H. R. Band, private communication.
- [7] S. R. Schaefer *et al.*, "Frequency Shifts of the Magnetic-Resonance Spectrum of Mixtures of Nuclear Spin-Polarized Noble Gases and Vapors of Spin-Polarized Alkali-Metal Atoms," *Phys. Rev.* **A39**, pp. 5613–5623, 1989.
- [8] Z-E. Meziani, private communication.
- [9] C. Y. Prescott *et al.*, "Parity Nonconservation in Inelastic Electron Scattering," *Phys. Lett.* **B77**, pp. 347–352, 1978.
- [10] G. Baum *et al.*, "A New Measurement of Deep Inelastic Electron-Proton Asymmetries," *Phys. Rev. Lett.* **51**, pp. 1135–1138, 1983.
- [11] D. Kawall *et al.*, "Large Volume Threshold Čerenkov Counters," presented at this symposium.
- [12] P. A. Souder, private communication.
- [13] H. Fonvieille, private communication.
- [14] G. T. Bartha *et al.*, "Design and Performance of the ASP Lead-Glass Calorimeter," *Nucl. Instr. Methods* **A275**, pp. 59–70, 1989.
- [15] K. L. Brown, "A First- and Second-Order Matrix Theory for the Design of Beam Transport Systems and Charge Particle Spectrometers," SLAC Report-75, 1982.
- [16] J. S. McCarthy and C. Y. Prescott, private communication.
- [17] C. Y. Prescott, private communication.

END

DATE
FILMED
02/13/92

